Preprints of the 19th World Congress
The International Federation of Automatic Control
Cape Town, South Africa. August 24-29, 2014

Coupling between the in-plane and lateral tape dynamics in high capacity linear tape transport systems

Hankang Yang and Sinan Müftü*

Department of Mechanical Engineering, Northeastern University, Boston, MA 02115 USA
(** Tel: 617-373-4743; e-mail: s.muftu@neu.edu*)

Abstract: Lateral tape motion (LTM) is defined as the lateral deviation of the tape from its prescribed strain-free state path. The effects of tape, roller, guide or reel imperfections on the LTM are reasonably well understood. Yet, the effects of disturbances in the longitudinal (in-plane) direction, which can couple into LTM, have not been well described. Longitudinal tape vibrations can be due to, but not limited to a) tension dynamics due to servo control of the tape reels, and/or tension impulses due to the unwinding of tape layers that experience sticking. The problem is further complicated due to the uncertainty of the tape length on the downstream side, as a result of the "floating layers" in the take-up reel. In this work, the equations of motion of the longitudinal and lateral tape motion are derived from first principles. The coupling due to non-linear longitudinal strain is considered. The equations of motion are solved by using the finite element method, and an explicit time integration algorithm. The entire tape path is modeled directly, where the interaction of the tape with the recording head and the guides are represented as concentrated forces, and moments. The effects of disturbances, typical for a tape transport system, on the coupling or lack there off are investigated.

1. INTRODUCTION

Lateral tape motion (LTM) can be described as deviation of the tape from its prescribed path, in the plane of the tape, in the lateral direction. Any imperfections in the alignment of the rollers, fixed guides, read-write (RW) heads, and tape reels, as well as the small and random variations in the tape width can cause LTM.

The effects of such imperfections have been modeled extensively by using a linear steady state model (Raeymaekers and Talke, 2009a, Raeymaekers et al., 2007, Raeymaekers and Talke, 2007, Raeymaekers and Talke, 2009b) and a linear transient model (Brake and Wickert, 2010a, Kartik and Wickert, 2008b). In practice the effects of LTM can be handled by moving the RW-head laterally, with a servo-control strategy that follows magnetic servo-tracks pre-written on the tape (Brake and Wickert, 2010a).

On the other hand, the effects of the events that cause sudden or random changes in tape tension have not been well understood (Anonymous, 2012). Longitudinal tape vibrations can be caused by various effects. For example, micro-slip between a smooth tape and a RW-head can cause scrape flutter. During start-up, the tape that has been stuck on a head, or a pack layer can suddenly release a tension wave, which will propagate through the tape path with unknown consequences. Such tension or transport speed fluctuations could cause parametric resonance. Several efforts have been made to understand such nonlinear, parametrically excited systems (Chen et al., 2010, Kartik and Wickert, 2008a, Mockensturm and Guo, 2005, Parker and Lin, 2001, Zhang and Zhu, 1999b, Zhang and Zhu, 1999a). However, these works were restricted to very simple tape drive layouts.

Tension and transport speed control were also studied related to lateral tape motion (Raeymaekers and Talke, 2009b, Shelton, 1968, Young et al., 1989, Sievers, 1987, Aravind and Pagilla, 2010) and simple stretch in longitudinal direction (Branca et al., 2013, Lee et al., 2010). A model that couples deflection in these two directions has not been developed.

In this paper a comprehensive mathematical model that is capable of predicting the in-plane tape dynamics and its cross-coupling to LTM with variety disturbances is introduced.

2. MODELING

Fig. 1 shows schematic depictions of a typical tape path and the definitions of the deflection components *u, v, w* with respect to a fixed Cartesian coordinate system (*x*, *y*, *z*), where *x*-, *y*- and *z*- axes represent the longitudinal, lateral and out-of plane directions. The tape is assumed to be translating in the longitudinal direction with transport velocity V_x. Each one of the deflection components is a function of (*x*, *t*). The strain free configuration of the tape follows an idealized path between the two reels with perfectly aligned components. Tape mechanics is analyzed in an unwrapped, straight configuration, and the effects of the various guides and the reels are imposed with appropriate external forces and boundary conditions, respectively (Brake and Wickert, 2010a). In this paper, we focus on the coupling between the in-plane $u(x,t)$ and the lateral tape deflection $v(x,t)$. The tape is modeled as a translating beam that can stretch in the in-plane direction. The longitudinal strain ε_{xx} in the tape is represented as follows (Nayfeh and Mook, 1979, Reddy, 2004, Wickert, 1992),

$$\varepsilon_{xx} = \frac{\partial u}{\partial x} + \frac{1}{2}\left(\frac{\partial v}{\partial x}\right)^2 - y\left(\frac{\partial^2 v}{\partial x^2}\right) \tag{1}$$

The extended Hamilton's principle, given as follows, is used to obtain the equation of motion,

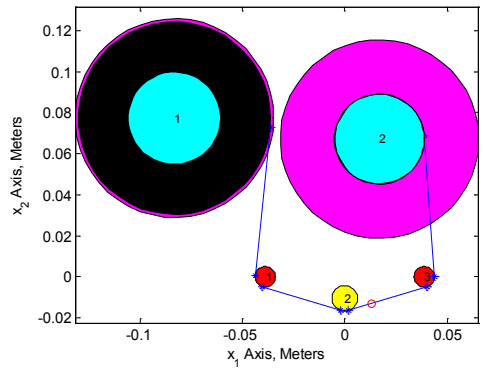

a)

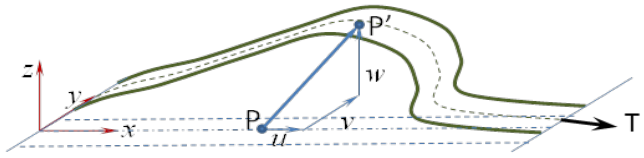

b)

Fig. 1. a) Schematic diagram of the tape path with supply (1) and take-up reels, two cylindrical guides (1,3) and a cylindrical head (2) depicted in drive base coordinates ($x1$, $x2$). b) Schematic diagram of the longitudinal, lateral and out-of-plane tape deflections.

$$\int_{t_1}^{t_2}\left(\delta K-\delta U+\delta W\right)dt=0 \tag{2}$$

where δK, δU and δW represent the variations of the kinetic energy, the strain energy, and the work done on the system, defined in the usual sense of the variational calculus, respectively (Reddy, 2004). The details of the derivation are omitted here. However, it should be mentioned that the viscoelastic nature of the polymeric tape material is considered. The constitutive behaviour for a translating viscoelastic string is given as follows (Mockensturm and Guo, 2005),

$$\sigma_{xx}=E\varepsilon_{xx}+\eta\frac{D\varepsilon_{xx}}{Dt} \tag{3}$$

where σ_{xx} is the longitudinal stress in the tape, and E and η are the elastic and loss moduli, respectively. The motion is observed in an Eulerian reference frame, therefore the material time derivative is used,

$$\frac{D(\bullet)}{Dt}=\frac{\partial(\bullet)}{\partial t}+V_x\frac{\partial(\bullet)}{\partial x} \tag{4}$$

Equation of motion of a translating tape is found as follows,

$$\rho A\frac{D^2u}{Dt^2}-\frac{\partial}{\partial x}\left(EA\varepsilon_{xx}+\eta A\frac{D\varepsilon_{xx}}{Dt}\right)=\sum_{i=1}^{N^g}f_{x_i}^g\delta\left(x-L_{g_i}\right) \tag{5}$$

$$\rho A\frac{D^2v}{Dt^2}-\frac{\partial}{\partial x}\left[A\left(E\varepsilon_{xx}+\eta\frac{D\varepsilon_{xx}}{Dt}\right)\frac{\partial v}{\partial x}\right]+\frac{\partial^2}{\partial x^2}\left[I_{zz}\left(E\frac{\partial^2v}{\partial x^2}+\eta\frac{D}{Dt}\left(\frac{\partial^2v}{\partial x^2}\right)\right)\right]=\sum_{i=1}^{N^g}f_{y_i}^g\delta\left(x-L_{g_i}\right) \tag{6}$$

where $\vec{f}_i^{\,g}$ $(i=1,N^g)$ represents the forces acting on the tape due to guides, each located at $x=L_{g_i}$, N^g is the total number of guides, and $\delta(x)$ is the Dirac delta function, not to be confused with the variational symbol in (2). In this work the guides are modelled as non-rotating, cylindrical supports. Therefore, the external forces acting on the tape contain contributions due to sliding friction. In addition, the aggregate effect of the tape's resistance to lateral motion over a guide is represented as a linear spring force (Brake and Wickert, 2010b, Yang. and Muftu., 2012) This gives the following force vector components,

$$f_{x_i}^g=-T_{0_i}\frac{Du/Dt+V_x}{\sqrt{\left(Du/Dt+V_x\right)^2+\left(Dw/Dt\right)^2}}\left(e^{\mu_x\theta_{wi}}-1\right) \quad \text{a)}$$

$$f_{y_i}^g=-T_{0_i}\frac{\mu_{y_i}}{\mu_{x_i}}\frac{Dw/Dt}{\sqrt{\left(Du/Dt+V_x\right)^2+\left(Dw/Dt\right)^2}}\left(e^{\mu_x\theta_{wi}}-1\right)+k_{g_i}w\left(L_{g_i}\right) \quad \text{b)} \tag{7}$$

where the subscript–i indicates the guide number, T_{0_i} is the tape tension upstream of the guide, μ_{x_i} and μ_{y_i} are the friction coefficients, θ_{w_i} is the wrap angle, and k_{g_i} is the guide stiffness.

The coupled equation of motion is solved numerically; lateral deflection is interpolated by piecewise continuous third-order, Hermite polynomials; longitudinal deflection is interpolated by piecewise continuous linear polynomials; explicit version of Newmark's time integration method is used for time discretization (Cook *et al.*, 2011). The details of the derivation, which leads to the following matrix representation of the coupled equation of motion, are omitted,

$$[M]\{\ddot{d}\}+[G]\{\dot{d}\}+[K]\{d\}=\{f\} \tag{8}$$

where [M], [G], and [K] are the mass, gyroscopic damping, and structural stiffness matrices, respectively, $\{d\}$, $\{\dot{d}\}$, $\{\ddot{d}\}$ and $\{f\}$ represent the displacement, velocity, acceleration and external forces at each point of the discretized continuum, respectively. A mesh convergence study and a verification test are presented in Appendix-A and –B, respectively.

3. RESULTS AND DISCUSSION

In this paper we investigate generation of LTM due to dynamic events that are predominantly in-plane.

In what follows, the tape width and thickness are 12.7 mm and 6.4 µm, respectively. The elastic modulus of the tape is 5 GPa, and it is calculated as described by (Brake and Wickert, 2010a). The loss modulus of the tape is 13 kPa.s. The lengths of the free tape-span between the two reels (Fig. 1) are 6.26, 4, 4, and 6.9 cm, respectively. The guide radii are 5, 6.2 and 5 mm, with wrap angles of 78.9, 33.8, and 77.2 degrees, respectively. The pack radii are 4.7 and 2.2 cm. The guide

stiffness values are 10, 0, and 100 N/m. In this work we accommodate for the floating tape layers in the take-up reel (Keshavan and Wickert, 1997) by extending the length of the tape between the guide-3 and reel-2 by integer multiples of $2\pi R_{R2}$, where R_{R2} is the current radius of the take-up pack.

3.1 LTM due to an Impulsive Change in Tension

There are several effects that can cause a sudden change in tape tension. For example, as the tape is unwound at the supply reel, the wound-in stress in the circumferential direction of the pack needs to adjust to the tension of the tape path. In this paper, we model the effect of such sudden changes in tension by applying a square tension impulse at the supply reel ($x = 0$) as follows,

$$T_b(0,t) = \begin{cases} T_0 & \text{for} \quad 0 \le t \le t^* \\ (1+r)T_0 & \text{for} \quad t^* \le t \le t^* + \tau^* \\ T_0 & \text{for} \quad t > t^* + \tau^* \end{cases} \tag{9}$$

where r is the tension amplitude ratio (r > -1) and the duration of impulse is τ^*. The effects of these two variables are investigated in the following range $-0.5 \le r \le 0.5$ and for τ^* = 5, 10, and 15 ms. The other boundary conditions of the system are prescribed as follows,

$$w(0,t) = w_0, \ \frac{\partial w}{\partial x}(0,t) = \psi_0 \tag{a}$$

$$u(L_b,t) = 0, \ w(L_b,t) = V_x \psi_L, \ \frac{\partial w}{\partial x}(L_b,t) = \dot{\psi}_L \tag{b) (10}$$

where w_0 and Ψ_0 represent a static tilt at the supply reel (x = 0), and (10b) represents the *Shelton boundary condition* at the take-up reel ($x = L_b$) (Brake, 2007, Benson, 2002, Shelton and Reid, 1971). Note that non-zero w_0 or Ψ_0 are very commonly encountered in realistic drive conditions, and also such values are necessary in order to seed lateral motion to the tape response, in the solution approach of this paper.

Fig. 2 shows the calculated longitudinal and lateral tape deflection histories monitored at the head (guide-2) position, for r = 0.5 and τ^*=15 ms. Fig. 2a shows that the in plane displacement component experiences two sudden changes at the onset and end of the square wave impulse, which causes high frequency (2066 Hz), in plane vibration with maximum amplitude of ~35 and 20 µm, respectively. As a consequence of this in plane action, vibration in the lateral direction is excited as shown in Fig. 2b. This vibration shifts the tape by ~25 nm in the lateral direction, at the location of the head. The primary frequency of the vibration shown in Fig. 2b is 666 Hz.

In the course of this investigation it was found that, for a fixed r value, the maximum tape deflection is independent of the duration of the impulse, τ^*. Therefore, in Fig. 3 we only present the effect of r on the maximum tape deflection for τ^* = 15 ms. This figure shows that the maximum tape deflection is a linear function of r. The static tilt angle at supply reel is responsible for the unequal slopes in Fig. 3b for the positive and negative r-values.This linear behaviour in this nonlinear system is due to the definition of longitudinal strain in (1), which in this case is dominated by $\partial u / \partial x$, due to the nature of the input. This in turn ends up dominating the longitudinal and lateral responses. It is also important to notice that when a lateral deflection is the source of energy input into the system, a linear relationship of the kind described above is not expected. In that case, a larger lateral motion is expected to enhance the nonlinearity. But, this is beyond the scope of the current investigation.

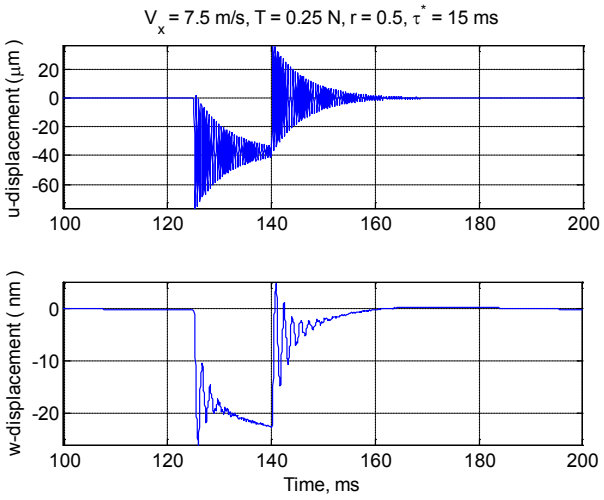

Fig. 2. Tape's longitudinal (top) and lateral (bottom) dynamics in response to a tension impulse T_0 = 0.25 N, r = 0.5, t^* = 125 ms, and τ^* = 15 ms, at V_x = 7.5 m/s.

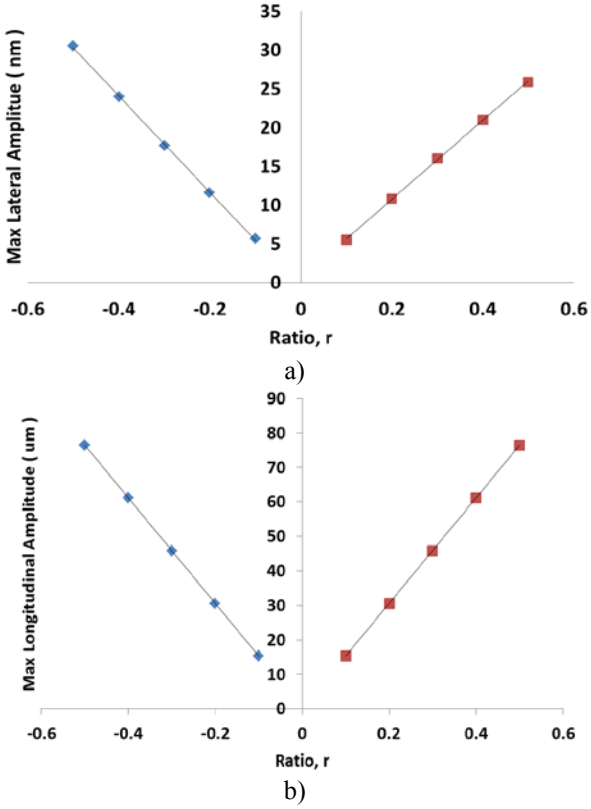

Fig. 3. Maximum tape deflection in a) lateral and b) longitudinal directions, in response to a tension impulse T_0 = 0.25 N, r = -0.5 - 0.5, t^* = 135 ms, τ^* = 15 ms, V_x = 7.5 m/s.

3.2 LTM due to Tension Dynamics

In a typical tape drive, the tape speed servo action causes tension fluctuations, even at steady state operating conditions (Koç et al., 2002, Mathur and Messner, 1998). In order to investigate the effects of the in plane tension fluctuations on the LTM, the system of equations are solved with a simple harmonic tension variation, $T_{b0}(t)$. The following boundary conditions are used,

$$T_b(0,t) = T_0\left(1 + r\sin\left(2\pi\Omega_T t\right)\right), w(0,t) = w_0, \frac{\partial w}{\partial x}(0,t) = \psi_0 \quad \text{(a)}$$

$$u(L_b,t) = 0, \quad w(L_b,t) = V_x\psi_L, \quad \frac{\partial w}{\partial x}(L_b,t) = \dot{\psi}_L \qquad \text{(b) (11)}$$

where Ω_T is the frequency of tension fluctuation applied at the supply reel ($x = 0$).

The tension fluctuation frequency is swept in the range $0 \leq \Omega_T \leq 5$ kHz, with relatively coarse increments of 100 Hz. Near the peaks the increments are reduced to 10 Hz. Simulations are carried out with parameter values that are relevant for the technological application: $T_0 = 0.25$, 0.5, and 0.75 N; $V_x = 2.5$, 5.0, and 7.5 m/s (Anonymous, 2012); and, with 0, 1 and 2 floating layers.

Fig. 4 shows the frequency response of the in-plane and lateral tape motions for three different tape transport velocities. In this frequency range, the tape has a single resonant frequency in its in-plane dynamics, around 2100 Hz as shown in Fig. 4a. This is close to 2250 Hz, obtained from $(E/\rho)^{1/2}/4L_b$, which is found for a non-travelling string with fixed-free boundary conditions. In response to tension fluctuations, three resonant peaks are excited in the lateral direction. These peaks are located around 700, 2100 and 3000 Hz. Transport velocity affects not only the damping in the system, but also the stiffness due to the inherent nature of the gyroscopic behaviour as expressed in the material time derivative of (3). In fact, increasing tape velocity raises the Coriollis acceleration, and eventually decreases damping and stiffness of the tape. The natural frequency and amplitudes of the lateral component of tape deflection increase, as a result of increasing the tape velocity from 2.5 m/s to 7.5 m/s. No significant frequency shift is observed at the second resonant frequency, but the response amplitude increases. A vibration mode in the lateral motion is excited around 2950 Hz. This mode absorbs increasingly more energy with increasing tape velocity. Also note that only one resonant frequency is coincident in both in-plane and lateral directions.

The effect of mean tension, T_0, on the resonant frequencies of the system is shown in Fig. 5. This result shows a clear coupling between the two vibration directions. Magnitude of the mean tension does not change the natural frequency of vibration in the longitudinal direction as shown in Fig. 6a. However, energy absorbed into the in-plane vibrations by the system increases with mean tension. The longitudinal strain couples the in-plane and lateral deflections, as shown in (6). Increasing tension stiffens the tape in the lateral direction, and results in increasing resonant frequencies of the lateral vibration modes.

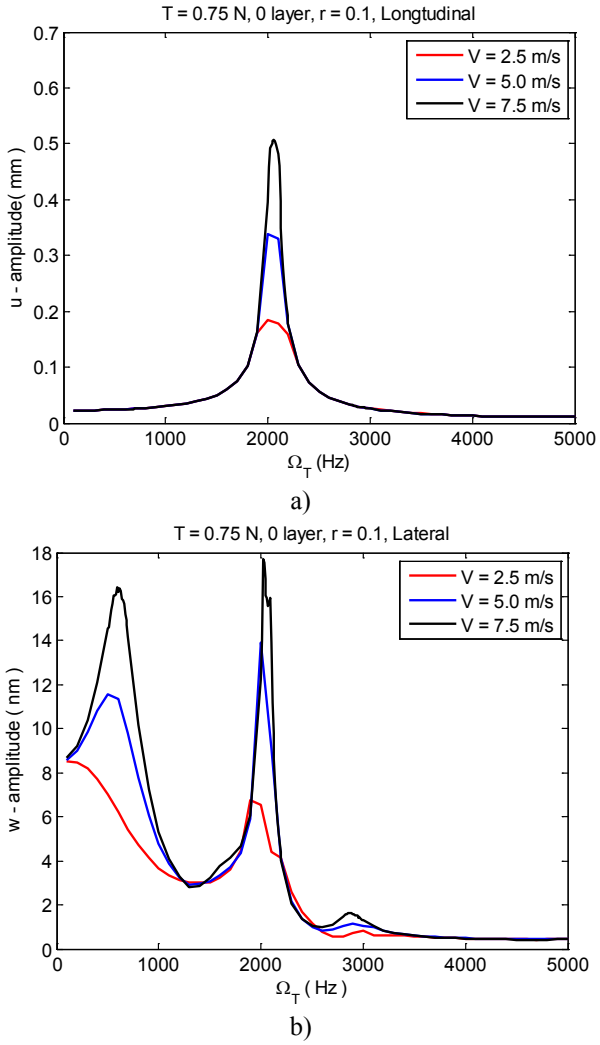

Fig. 4. Frequency spectra in a) lateral and b) longitudinal directions, for tape at different tape transport velocitys, V_x = 2.5, 5.0, and 7.5 m/s with T = 0.75 N, r = 0.1, and zero floating layers.

This increase is small at the natural frequency, but it can be seen more clearly at around 2,800 Hz (fourth resonant frequency). Also note that a resonant frequency around 1,600 Hz appears for the T_0 = 0.25 N. This frequency is merged with the third natural frequency for higher tension values.

The effect of the floating layers in the take-up pack is analysed for 0, 1 and 2 layers. Floating layers increase the tape span. In order to stay consistent in numerical analysis, the element size is kept constant, but the number of elements is increased. Fig. 6 shows that the increasing number of floating layers dramatically reduces the resonant frequencies of the in-plane and lateral tape dynamics. Both lateral and longitudinal vibration resonant frequencies move to lower values with increasing number of layers. In spite of using a sampling rate of 10 Hz in the 100 - 1000 Hz range, the frequency spectrum of the case of 2 layers shows sharp variations in Fig. 7b. Increasing the number of layers adds more resonant frequency values into the 5 kHz range. This result is attributed to the fact that longitudinal and lateral tape vibrations have natural frequencies proportional to the reciprocal of total tape length.

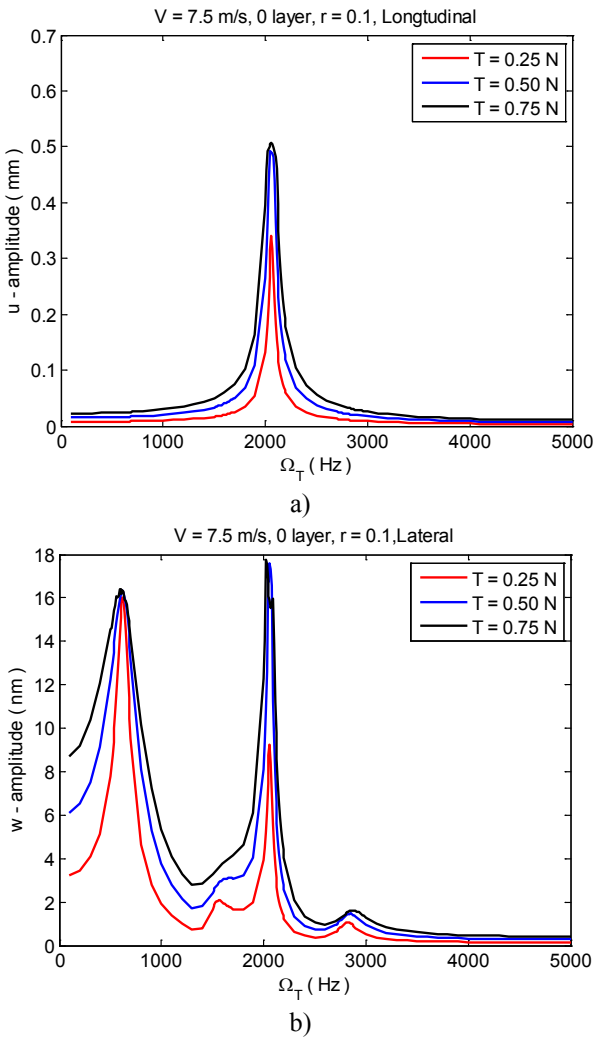

Fig. 5. Frequency spectra in a) lateral and b) longitudinal directions, for tape at under $T = 0.25$, 0.5, and 0.75N tension with, $V_x = 7.5$ m/s $r = 0.1$, and zero floating layers.

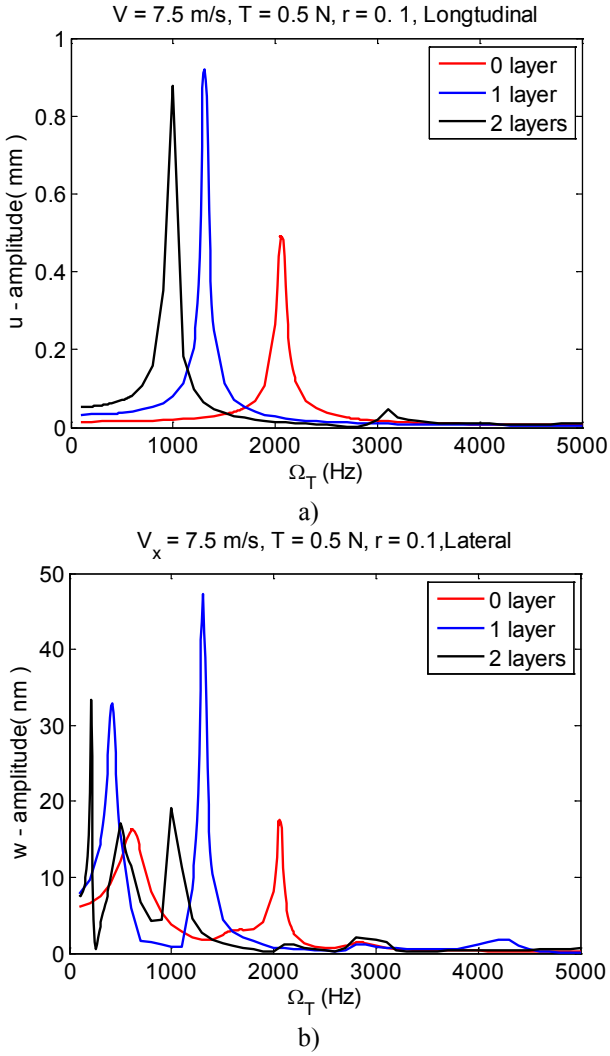

Fig. 6. Frequency spectra in a) longitudinal and b) lateral directions for tape with 0, 1 and 2 floating layers at the take-up pack, with $V_x = 7.5$ m/s, $T = 0.5$ N, and $r = 0.1$.

4. SUMMARY AND CONCLUSIONS

Equation of motion of a tensioned tape, translating between two reels, and supported by friction guides is presented. In particular the non-linear coupling between the in-plane and lateral tape deflection components is modelled. The coupling is investigated for two scenarios that are common in current tape drive systems: a) tension impulse due to mismatch of in-plane stresses in the reel and the tension on the tape-path; and b) tension fluctuations due to tape–speed servo control.

It was shown that the tension impulse can cause a high frequency high amplitude wave in the in-plane direction, and also excites lateral motion. The effect of the in-plane wave can potentially cause local stretching of the bits.

The amplitude of the in-plane and lateral deflections due to tension impulse varies linearly with the impulse strength. It was also shown that the tension fluctuation, which primarily affects the in-plane tape deflection, can excite resonances in the lateral tape motion. Tape velocity and tension have relatively small effects on the resonant frequencies in the range considered, but deflection amplitudes increase with increasing values of T_0 and V_x, as expected. On the other hand, the increasing number of floating layers on the take-up pack lower the natural frequencies and "invite" more resonances into the 0 - 5 kHz range. Possibility of parametric resonance should be included in high capacity data tape drive design.

REFERENCES

ANONYMOUS 2012. International Magnetic Tape Storage Technology Roadmap, 2012-2022.

ARAVIND, S. & PAGILLA, P. R. 2010. Optimal Web Guiding. *Journal of Dynamic Systems, Measurement, and Control,* 132**,** 011006-1-011006-10.

BENSON, R. C. 2002. Lateral Dynamics of a Moving Web With Geometrical Imperfection. *Journal of Dynamic Systems, Measurement, and Control,* 124**,** 25.

BRAKE, M. R. & WICKERT, J. A. 2010a. Lateral Vibration and Read/Write Head Servo Dynamics in Magnetic

Tape Transport. *Journal of Dynamic Systems and Control,* 132.

BRAKE, M. R. & WICKERT, J. A. 2010b. Tilted Guides with Friction in Web Conveyance Systems. *International Journal of Solids and Structures,* 47**,** 2952-2957.

BRAKE, M. R. W. 2007. *Lateral Vibration of Moving Media with Frictional Contact and Nonlinear Guides.* PhD, Carnegie Mello University.

BRANCA, C., PAGILLA, P. R. & REID, K. N. 2013. Governing Equations for Web Tension and Web Velocity in the Presence of Nonideal Rollers. *Journal of Dynamic Systems, Measurement, and Control,* 135**,** 011018-1-011018-10.

CHEN, L.-Q., TANG, Y.-Q. & LIM, C. W. 2010. Dynamic Stability in Parametric Resonance of Axially Accelerating Viscoelastic Timoshenko Beams. *Journal of Sound and Vibration,* 329**,** 547-565.

COOK, R. D., MALKUS, D. S., PLESHA, M. E. & WITT, R. J. 2011. *Concepts and Applications of Finite Element Analysis,* New Jersey, John Wiley & Sons.

KARTIK, V. & WICKERT, J. A. 2008a. Parametric Instability of a Traveling Plate Partially Supported by a Laterally Moving Elastic Foundation. *Journal of Vibration and Acoustics,* 130**,** 051006.

KARTIK, V. & WICKERT, J. A. 2008b. Surface Friction Guiding for Reduced High-Frequency Lateral Vibration of Moving Media. *Journal of Vibration and Acoustics,* 129**,** 371-379.

KESHAVAN, M. B. & WICKERT, J. A. 1997. Air Entrainment During Steady-State Web Winding. *ASME J. Appl. Mech,* 64**,** 916-922.

KOÇ, H., KNITTEL, D., DE MATHELIN, M. & ABBA, G. 2002. Modeling and Robust Control of Winding Systems for Elastic Webs. *IEEE Transactions on Control Systems Technology,* 10**,** 197-208.

LEE, G. T., SHIN, J. M., KIM, H. M. & KIM, J. S. 2010. A Web Tension Control Strategy for Multi-span Web Transport Systems in Annealing Furnace. *ISIJ International,* 50**,** 854-863.

MATHUR, P. D. & MESSNER, W. C. 1998. Controller Development for a Prototype High-Speed Low-Tension Tape Transport. *IEEE Transactions on Control Ssytems Technology,* 6**,** 534-542.

MOCKENSTURM, E. M. & GUO, J. 2005. Nonlinear Vibration of Parametrially Excited, Viscoelastic, Axially Moving Strings. *Journal of Applied Mechanics,* 72**,** 374-380.

NAYFEH, A. H. & MOOK, D. T. 1979. *Nonlinear Oscillations,* New York, USA, Wiley.

PARKER, R. G. & LIN, Y. 2001. Parametric Instability of Axially Moving Meida Subjected to Multifrequency Tension and Speed Fluctuations. *Journal of Applied Mechanics,* 68**,** 49-57.

RAEYMAEKERS, B., ETSION, I. & TALKE, F. E. 2007. Influence of operating and design parameters on the magnetic tape-guide friction coefficient. *Tribology Letters,* 25**,** 161-171.

RAEYMAEKERS, B. & TALKE, F. E. 2007. Lateral Motion of an Axially Moving Tape on a Cylindrical Guide Surface. *Journal of Applied Mechanics,* 74**,** 1053.

RAEYMAEKERS, B. & TALKE, F. E. 2009a. Attenuation of LTM due to frictional inteaction with a cylindrical guide. *Tribology International,* 42**,** 609-614.

RAEYMAEKERS, B. & TALKE, F. E. 2009b. Measurement and Sources of Lateral Tape Motion: A Review. *Journal of Tribology,* 131**,** 011903.

REDDY, J. N. 2004. *An introdunction to nonlinear finite element analysis,* United State, OXFORD.

SHELTON, J. J. 1968. *Lateral Dynamics of A Moving Web.* Ph.D, Oklahoma State University.

SHELTON, J. J. & REID, K. N. 1971. Lateral Dynamics of an Idealized Moving Web. *Journal of Dynamic Systems, Measurement, and Control,* 93**,** 187-192.

SIEVERS, L. A. 1987. *Modeling and Control of Web Conveyance Systems.* Ph.D, Rensselaer Polytechnic Institute.

WICKERT, J. A. 1992. Non-Linear Vibration of a Traveling Tensioned Beam. *International Journal of Non-Linear Mechanics,* 27**,** 503-517.

WICKERT, J. A. & MOTE JR, C. D. 1990. Classical vibration analysis of axially moving continua. *Journal of Applied Mechanics,* 57**,** 738-744.

YANG., H. & MUFTU., S. 2012. Lateral Tape Dynamics over Non-Linear Guides. *2012 ASME-ISPS /JSME-IIP Joint International Conference on Micromechatronics for Information and Precision Equipment, MIPE2012.* Santa Clara, California, USA.

YOUNG, G. E., SHELTON, J. J. & KARDAMILAS, C. 1989. Modeling and Control of Mutiple Web Spans Using State Estimation. *Journal of Dynamic Systems, Measurement, and Control,* 111**,** 505-510.

ZHANG, L. & ZHU, J. W. 1999a. Nonlinear Vibration of Parametericlly Excited Moving Belts, Part I: Dynamic Response. *Transactions of the ASME,* 66**,** 396-402.

ZHANG, L. & ZHU, J. W. 1999b. Nonlinear Vibration of Parametrically Excited Viscoelastic Moving Belts, Part II: Stability Analysis. *Journal of Applied Mechanics,* 66**,** 403-409.

APPENDIX-A

Mesh convergence is carried out for the geometry described in Fig. 1, without any guides. The supply pack is tilted by 0.1 mrad, and an impulse is applied in the tensile direction from the supply pack. The amplitude of the impulse is $1.2T_0$ with duration of 15 ms. The mean tension is 0.25 N, and the tape velocity is 7.5 m/s. Dynamics of the mid-point of the tape span is monitored for different number of elements (20, 30, 40, 50 and 60) and time step sizes (5, 10, 50 ns). Results are compared in Fig. 7. The change in the predicted response by increasing the number of elements from 20 (blue solid line) to 30 (blue dash-dot line) is significant. The change is much less from 40 elements to 60. The difference between the 50 (blue dashed line) and 60 (blue dashed line) elements is within 1 nm. In this study, 50 elements, with corresponding

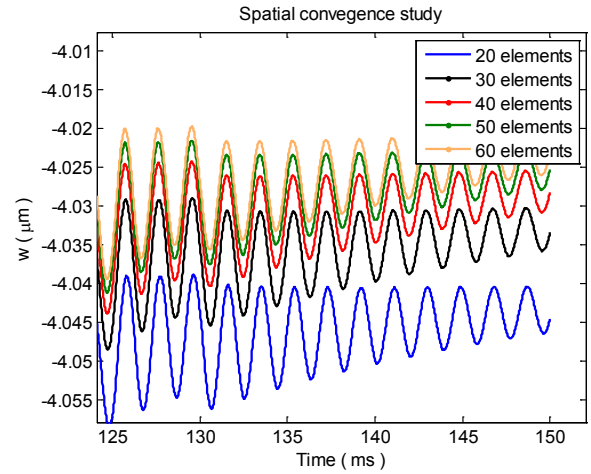

a)

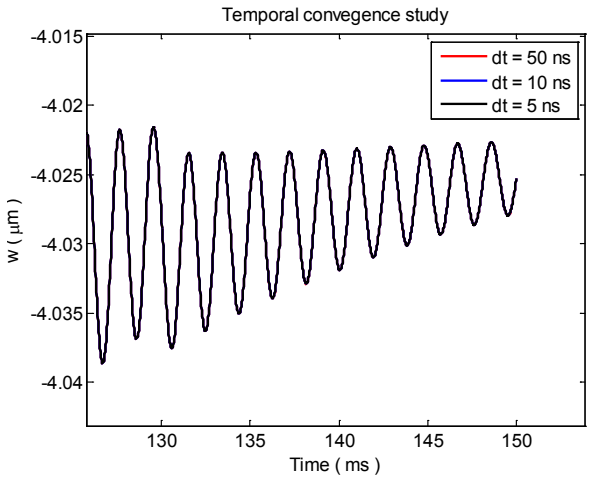

b)

Fig. 7. Convergence study for testing the effects of a) the mesh size, Δx , and b) the time increment, Δt .

length of $\Delta x = 4.77$ μm, is used. The temporal convergence study shows (Fig. 7b) that the results are virtually identical for all three time step sizes. In the rest of this study $\Delta t = 10$ ns is used.

The effectiveness of the numerical approach to predict the classical results is investigated for the case of constant tension. The longitudinal stress is modified as follows,

$$\sigma_{xx} = \frac{T_0}{A} + E\varepsilon_{xx} + \eta \frac{D\varepsilon_{xx}}{Dt} \tag{12}$$

The same numerical approach outlined above is used for a tape translating between two supports. Equations (5) and (6) are subjected to following boundary conditions,

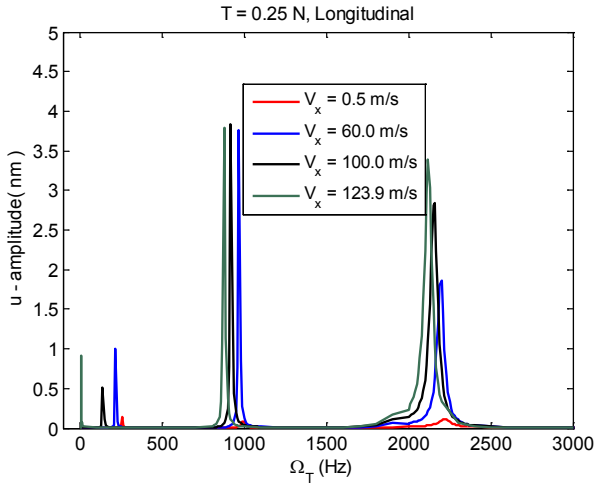

a)

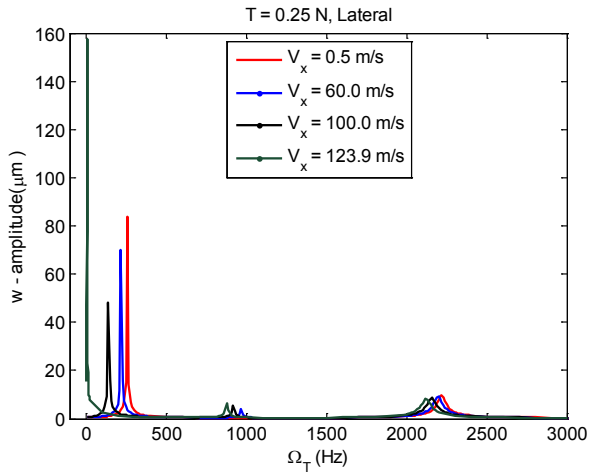

b)

Fig. 8. Frequency response of the tape traveling between two supports for different tape transport speeds.

$$u(0,t) = 0 \text{ and } u(L_b,t) = 0 \tag{a}$$

$$w(0,t) = w_0 \sin(2\pi\Omega_T t), \text{ and } \frac{\partial^2 w}{\partial x^2}(0,t) = 0 \tag{b}$$

$$w(L_b,t) = 0 \text{ and } \frac{\partial^2 w}{\partial x^2}(L_b,t) = 0 \tag{c}$$

A frequency sweep in the range $0 \le \Omega_T \le 3$ kHz is conducted for $w_0 = 1$ μm, for different tape transport speeds. Fig. 8 demonstrates the effects of velocity and tension on the natural frequencies. Fig. 8 shows that the natural frequencies decrease by increasing velocity for all the modes in the range investigated. This trend is consistent with (Wickert and Mote JR, 1990) who gives the critical transport velocity as $V_{xc} = 124.3$ m/s.